Strong transfer channels in the ^{6}Li+^{28}Si system at near-barrier energies

A. Pakou,[1] K. Rusek,[2] N. Alamanos,[3] X. Aslanoglou,[1] S. Harissopulos,[4] M. Kokkoris,[5] A. Lagoyannis,[4] T. J. Mertzimekis,[1] A. Musumarra,[6] N. G. Nicolis,[1] C. Papachristodoulou,[1] D. Pierroutsakou,[7] and D. Roubos[1]

[1]*Department of Physics, University of Ioannina, GR-45110 Ioannina, Greece*
[2]*Department of Nuclear Reactions, Andrzej Sołtan Institute for Nuclear Studies, Hoża 69, PL-00681 Warsaw, Poland*
[3]*DSM/DAPNIA CEA SACLAY, F-91191 Gif-sur-Yvette, France*
[4]*National Research Center Demokritos, Greece*
[5]*National Technical University of Athens, Greece*
[6]*Dipartimento di Metodologie Fisiche e Chimiche per l'Ingegneria dell'Universita di Catania, Italy*
[7]*INFN Sezione di Napoli, I-80125, Napoli, Italy*

(Received 30 May 2007; revised manuscript received 28 August 2007; published 7 November 2007)

Exclusive α-particle and proton production measurements of the system ^{6}Li+^{28}Si are performed at near-barrier energies. Each reaction channel is tagged via a particle-γ coincidence requirement. Ratios of direct to compound contributions are estimated via particle angular distribution measurements. Strong reaction channels for n and p transfer are identified and quantified and found to be described well on a qualitative basis with distorted-wave Born approximation calculations.

DOI: 10.1103/PhysRevC.76.054601 PACS number(s): 25.70.Bc, 24.10.Ht, 24.10.Lx, 24.50.+g

I. INTRODUCTION

The study of reaction mechanisms at near-barrier energies is a very popular playground, with recent emphasis on research concerning weakly bound nuclei. Approaching the vicinity of the Coulomb barrier, couplings between various channels play a major role in describing elastic scattering (potential threshold anomaly) or fusion (enhanced or reduced fusion cross sections). Thanks to systematic research on these topics with weakly bound nuclei, new phenomena have been recently revealed. With respect to the potential anomaly at the barrier a "new" anomaly has been pointed out recently on experimental grounds via new elastic scattering data and the reanalysis of older work for ^{6,7}Li on various targets [1–6], as well as on theoretical grounds via dispersion relations [7]. With respect to fusion, enhanced cross sections below the barrier [8–10] seek the appropriate theory to be validated. It has been suggested, from inclusive α-production cross section measurements [11–14], that couplings to breakup and transfer channels are the key issues for the above subjects. Earlier findings give the dominant role to breakup (see, e.g., Refs. [15,16]), while now this role is also given to transfer [17–19].

Either such couplings have to be taken into account via coupled channel theories or the energy dependence of the various optical model parameters has to be considered explicitly. In either case, the need for comprehensive studies is vital for all reaction channels involved at barrier energies. In this context, exclusive measurements recently performed [20–24] start to unfold a rather complicated situation. Contributing in this direction, we present in this letter, exclusive measurements on α and p production for the system ^{6}Li+^{28}Si at near-barrier energies. Particles are tagged by γ rays deexciting the exit channel nuclei. For the same system, exclusive measurements on breakup have already been reported [21], supporting very low cross sections. This system is therefore the most appropriate for probing coupled channel effects connected with transfer at near-barrier energies. Thus, the aim of this work is to identify and quantify the various transfer channels, estimating simultaneously the direct to compound contributions at selected near-barrier energies.

II. EXPERIMENTAL DETAILS AND DATA REDUCTION

^{6}Li^{3+} beams were delivered by the TN11/25 HVEC 5.5 MV Tandem accelerator of the National Research Center of Greece-DEMOKRITOS at two bombarding energies, namely, 9 and 13 MeV. Beam currents were of the order of 30 nA. The beam impinged on a 400 μg/cm^2 thick, self-supporting natural silicon target, in a target frame fixed parallel to the face of the detector. Reaction products were identified by a ΔE-E telescope set 12.7 cm from the target. The thickness of the ΔE silicon detector was 10 μm, while the thickness of the E detector was 2000 μm. The α and proton groups were well discriminated from the lithium ions by the ΔE-E technique.

To separate the direct from the compound contribution, particle angular distribution measurements were performed with the telescope, rotated in a D-shape chamber, in the angular range $\theta_{\rm lab} = 30^\circ$–$80^\circ$ for the 13 MeV experiment and $\theta_{\rm lab} = 35^\circ$–$70^\circ$ for the 9 MeV experiment. γ rays were observed by a 50% efficient Ge detector fixed at 90° with respect to the beam direction, 3.1 cm from the target. The efficiency of the Ge detector was determined via a ^{152}Eu source of known activity. Summing effects were estimated by placing the detector at various distances from the target as well as with a ^{22}Na source. The various reaction channels were tagged via a particle-γ coincidence requirement. γ-ray spectra in coincidence with α and proton particles are displayed for $E_{\rm lab} = 13$ MeV, in Figs. 1(a) and 1(b), respectively. γ rays of the most important exit channels (Table I) are appropriately marked. Particle spectra for one of these channels (^{29}Si), tagged by γ-ray ground state transitions ($3/2^+$ at 1.27 MeV $\rightarrow$ $1/2^+$ at 0 MeV, $5/2^+$ at 2.03 MeV $\rightarrow$ $1/2^+$ at 0 MeV, and $3/2^+$ at 2.43 MeV $\rightarrow$ $1/2^+$ at 0 MeV) are displayed in

TABLE I. Open channels in the reaction ^{6}Li+^{28}Si at beam energies 13 and 9 MeV. Total cross sections σ_T are obtained by integrating presently measured angular distributions. Evaporation cross sections σ_E are calculated values via the codes CASCADE and MECO (see text). Transfer cross sections $\sigma_D^{\rm exp}$ are values obtained by subtracting σ_T and σ_E. No error is assigned to the calculated values, estimated to be up to 4%. Last, the column under $\sigma_D{}^{\rm th}$ shows the n-, p-, and α-transfer calculations. For p transfer, a theoretical calculation with branching ratio equal to unity is presented in parentheses (see text). The symbol * indicates a very small cross section.

^{6}Li+^{28}Si →	$E_{\rm lab}$(MeV)	σ_T(mb)	σ_E(mb)	$\sigma_D^{\rm exp}$(mb)	$\sigma_D^{\rm th}$(mb)	σ_D/σ_E
^{29}Si+$\alpha+p$	13	355 ± 29	242	113 ± 29	37.9	0.47 ± 0.12
^{29}Si+$\alpha+p$	9	177 ± 10	70	107 ± 10	16.9	1.52 ± 0.14
^{32}S+$p+n$	13	270 ± 15	232	38 ± 15	4.5	0.16 ± 0.06
^{32}S+$p+n$	9	65 ± 3	72	*	0.8	
^{29}P+$\alpha+n$	13	46 ± 5	7	40 ± 5	19(36.5)	5.7 ± 0.09
^{29}P+$\alpha+n$	9	21 ± 1	0	21 ± 1	6.5	∞
^{28}Si+$\alpha+p+n$	13	22.0 ± 3.5	15	–	–	
^{28}Si+$\alpha+p+n$	9	0	0	–	–	

Fig. 2, for $\theta_{\rm lab}=30^\circ$. For each ground state transition and each element, such spectra were integrated, and the obtained yields normalized to the solid angle subtended by the telescope, the efficiency of the γ detector and the integrated charge. The charge was obtained from an analysis of the elastically scattered lithium ions, taking into account the well-known angular distribution, obtained from our previous experiment [1]. In general, total cross sections at each angle were obtained by summing the yield of particles, tagged with all the observed ground state transitions (see, e.g., Refs. [25,26]). We should, however, note that in the present study in this low energy regime, only one ground state transition is observed for all exit channels, except the ^{29}Si one, where three ground state transitions are observed. These transitions include cascades from higher states up to 3 and 6 MeV, depending on channel and beam energy. The above entry states are identified via our γ spectra and compound calculations. Losses due to direct feeding of the ground state are estimated to be of the order of 2% according to present compound calculations. These calculations are tested against reaction channels, which are formed purely via a compound process (for details, see Sec. III).

The angular distribution results are presented in Figs. 3 and 4. Exit channels considered in this work are displayed in Table I, together with their reaction cross sections, σ_T. These results were obtained by integrating our presently measured angular distribution cross sections, adopting the shape of the calculated angular distributions.

III. ANALYSIS OF THE DATA

To disentangle the compound from the direct part of the reaction cross sections and to obtain σ_E (compound cross sections)and σ_D (direct cross sections), we followed the method described in Ref. [17]. First, we estimated the compound contribution, and then we subtracted it from the data. The new values obtained are labeled "new data" and were handled as direct cross sections. Compound calculations

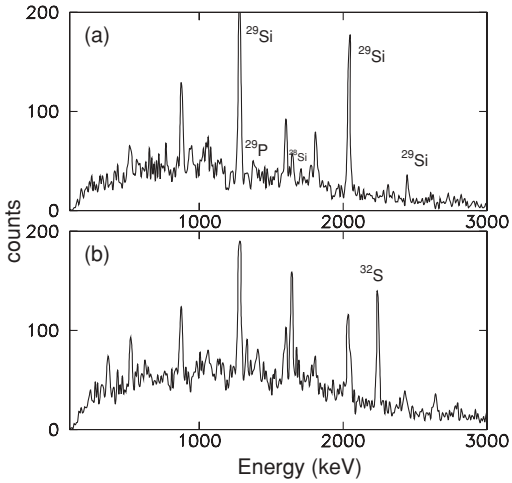

FIG. 1. γ-ray spectra gated with time to amplitude converter (TAC) and (a) α particles and (b) protons, produced in the ^{6}Li+^{28}Si reaction at $E_{\rm lab}=13$ MeV.

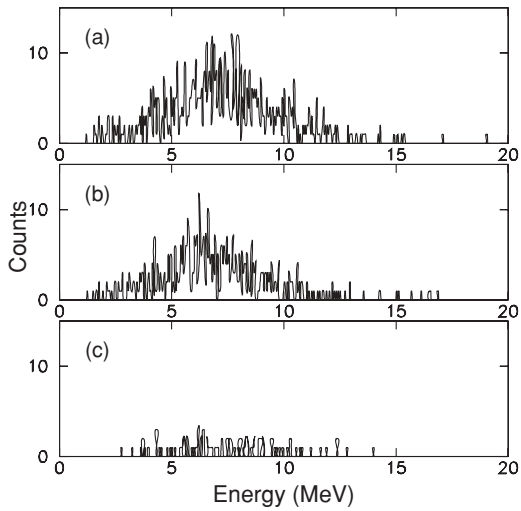

FIG. 2. α-particle spectra observed at $\theta_{\rm lab}=30^\circ$, gated with TAC and (a) the 1273 keV γ ray of ^{29}Si, (b) the 2028 keV γ ray of ^{29}Si, and (c) the 2426 keV γ ray of ^{29}Si.

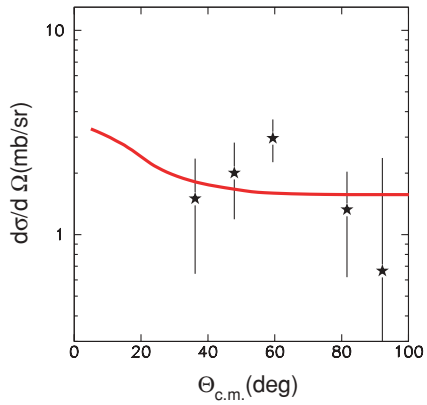

FIG. 3. (Color online) Experimental angular distribution (stars) compared with evaporation calculations (solid line) for the ^{6}Li+^{28}Si $\rightarrow$ ^{28}Si + α+p+n reaction at $E_{\text{beam}} = 13$ MeV (α-γ coincidences).

were performed with both the Monte-Carlo statistical model evaporation code MECO [1] and the code CASCADE [27]. The code MECO uses optical model transmission coefficients for particle emission and default γ-ray strengths as in the code PACE [28]. Level density parameters were obtained from the compilation of Gilbert and Cameron [29]. The excitation energy dependence and asymptotic high-energy limits of these parameters are given according to the ansatz of Ignatyuk [30]. Compound nucleus spin distributions were calculated with transmission coefficients obtained by a one-dimensional barrier penetration model using the Bass nuclear potential [31]. The code CASCADE was applied according to Ref. [27]. Level density parameters were constrained through the decay chain

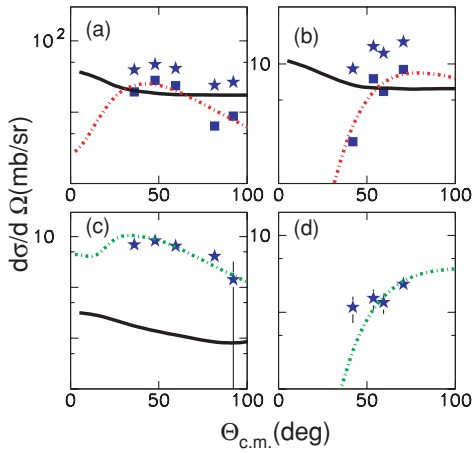

FIG. 4. (Color online) Experimental angular distributions (α-γ coincidence measurements) with compound and transfer calculations (see text) for the ^{6}Li+^{28}Si reaction and exit channels (a) and (b) ^{29}Si+α+p at $E_{\text{beam}} = 13$ and 9 MeV, respectively, and (c) and (d) ^{29}P+α+n at $E_{\text{beam}} = 13$ and 9 MeV, respectively. Stars represent the original data, while squares are the so-called new data (original data minus the compound cross sections). Solid lines represent our evaporation calculation; dotted-dashed lines, our DWBA calculation for n and p transfer. The transfer calculations had to be multiplied by factors of 3.5, 4.5, 2.2, and 4.5 for (a), (b), (c), and (d), respectively (see text), in order to best fit the data.

at the value $A/8$ MeV^{-1}. At low excitation energies, energy levels were introduced via the input file for each daughter nucleus. For the emission of electric dipole and quadrupole radiation and for the magnetic dipole radiation, a constant strength was used [32] as well as an energy dependence which is the basic energy dependence of single-particle transitions. The transmission coefficients for particle emission were obtained from the optical model using average parameters. The Bass nuclear potential combined with a one-dimensional barrier penetration model was used to fix the total cross section upper limit.

Angular distributions were obtained with the code MECO, while total fusion cross sections for each reaction channel were obtained with both codes MECO and CASCADE. The latter results are in very good agreement between themselves, suggesting that the calculation gives a good estimate of the compound formation cross section. Further support to this argument is given via our experimental data referring to the channel ^{6}Li+^{28}Si $\rightarrow$ ^{28}Si+α+p+n which proceeds only via a compound formation. Experimental and calculated cross sections with the code MECO are compared in Fig. 3 for the above-mentioned channel. The good agreement between experimental and calculated values for compound formation gives us the initiative to proceed with the analysis described above.

Results of the original angular distribution data and the "new data" ("new datum" at each angle equals the original datum at each angle minus the calculated compound contribution for this angle) are shown in Fig. 4 for the exit channels ^{29}Si+α+p and ^{29}P+α+n. It should be emphasized here that the nuclei ^{29}Si and ^{29}P can only be reached via complete fusion or transfer processes. Incomplete fusion, which is a major contributor to reactions of ^{6}Li with heavier targets [33], is ruled out from the present study on the the following grounds. While, in general, incomplete fusion cannot be disentangled from complete fusion because both processes lead to the same nuclei, here according to CASCADE calculations, the d+^{28}Si reaction leads to two nuclei, ^{26}Al and ^{25}Mg, unobtainable with complete fusion. γ rays deexciting these nuclei are not observed in our spectra, giving us the first evidence that incomplete fusion may not be present. No such evidence can be given for incomplete fusion of the α fragment, α+^{28}Si, where the produced nuclei coincide with those of complete fusion. In either case, however, the ^{29}Si and ^{29}P nuclei can be produced with incomplete fusion by the evaporation of protons and neutrons ($d + {}^{28}\text{Si} \rightarrow {}^{29}\text{Si} + p$, $d + {}^{28}\text{Si} \rightarrow {}^{29}\text{p} + n$, $\alpha + {}^{28}\text{Si} \rightarrow {}^{29}\text{P} + p + n + n$, and $\alpha + {}^{28}\text{Si} \rightarrow {}^{29}\text{Si} + p + p + n$). Providing that our measurements are restricted by an (α-γ) coincidence requirement, they exclude the observation of incomplete fusion, simplifying our study of complete fusion and transfer reactions.

The new data obtained after the subtraction represent direct reaction cross sections and specifically n transfer for ^{29}Si, p transfer for ^{29}P, and α transfer for ^{32}S. Total transfer cross sections for each channel are formed by integrating the angular distributions of the new data. The results are displayed in Table I under the column σ_D^{exp}. Ratios of transfer cross sections to the compound ones, where both reaction channels exist, are also shown in the last column of this table. From

TABLE II. Previous and present total reaction cross sections for ^{6}Li+^{28}Si at 13 and 9 MeV. $\sigma^{\rm tot}_{\rm prev.(el)}$ is the total cross section measured previously via elastic scattering, with $\sigma 1$ from Ref. [1] and $\sigma 2$ from Ref. [34]; $\sigma^{\rm tot}_{\rm prev.(dir)}$ is the total cross section measured previously via the direct technique [35]; and $\sigma^{\rm tot}_{\rm pres.}$ is the total cross section presently measured via α-γ measurement. This result includes missing channels due to evaporation and breakup (see text). Present total transfer cross sections (combining the results of Table I and a previous measurement on breakup, see text) are also included under the label $\sigma^{D-{\rm tot}}_{\rm pres.}$ and are compared with a previous measurement concerning direct processes at 13 MeV (see text). Ratios of transfer cross sections vs total cross sections presently measured are given in the last column.

Energy(MeV)	$\sigma 1^{\rm tot}_{\rm prev.(el)}$	$\sigma 2^{\rm tot}_{\rm prev.(el)}$	$\sigma^{\rm tot}_{\rm prev.(dir)}$	$\sigma^{\rm tot}_{\rm pres.}$	$\sigma^{D-{\rm tot}}_{\rm pres.}$	$\sigma^{D-{\rm tot}}_{\rm prev.}$	Ratio
13	954 ± 35	970 ± 70	940 ± 188	903 ± 38	221 ± 33	230 ± 30	0.24 ± 0.04
9	298 ± 25		412 ± 84	325 ± 14	118 ± 8		0.36 ± 0.03

these ratios it becomes apparent that when approaching the barrier, transfer channels become stronger than the compound ones. Another point to be discussed here is about missing channels not reported in Table I. According to our CASCADE calculations, such channels lead to ^{33}S and ^{32,31,30}P, with ^{32}P most prominent. The ^{31}P nucleus is produced with a very low cross section $\leqslant$6 mb, while the remaining nuclei are radioactive with very long lifetimes and therefore are unobserved in our measurements. Cross section calculations for these channels sum to 180 and 62 mb for 13 and 9 MeV, respectively. Taking into account observed (Table I) and missing channels (missing channels due to evaporation mentioned above and due to breakup amounting up to $\sim$30 mb, as measured previously [21]), we obtain total reaction cross sections of 900$\pm$38 mb for 13 MeV and 325$\pm$14 mb for 9 MeV. These results are compared in Table II with previous values obtained via elastic scattering [1,34] and other direct techniques [35]. Combining the results of Table I and the breakup cross section, total transfer cross sections are formed and included in Table II. Our measurement at 13 MeV is compared with a previously existing value concerning the cross section of direct reactions. In the same table, we present ratios of transfer cross sections vs total reaction cross sections determined in this study (last column). From these ratios, it is obvious that transfer channels are strong at near-barrier energies.

IV. TRANSFER CALCULATIONS

To compare our transfer results with theory, we performed distorted-wave Born approximation (DWBA) calculations for the n, p, and α transfer reactions induced by a ^{6}Li beam on ^{28}Si at the two energies, 9 and 13 MeV. We have not considered d transfer, because it leads to ^{30}P, which is unobservable in the statistics of the present experiment. This channel due to its very high Q value (+10.4 MeV) can proceed with substantial cross section only to high excitation states near the breakup threshold of ^{30}p$\rightarrow$ ^{28}Si+d, but the discrete states in this region are not known to make any further speculations. Details of the n-, p-, and α- transfer calculations are given below.

A. *n* -transfer DWBA calculations

To reproduce the data, we studied one-neutron transfers to ten of the excited states of the final nucleus, three as listed in the experimental details and seven at higher excitation energies that subsequently γ-decay to those three (such decays are confirmed in our γ spectra). States with the higher spectroscopic amplitudes are chosen [36].

The parameters used in the DWBA calculations are as follows. In the entrance channel ^{6}Li+^{28}Si optical model potentials are used which reproduce the elastic scattering at 9 and 13 MeV very well. They are obtained from the continuum-discretized coupled channels (CDCC) calculations described in Ref. [1]. The potentials in the exit channel are derived from proton-^{29}Si and α-^{29}Si optical model potentials at relevant energies by means of the single-folding technique. The proton-^{29}Si potential was taken from the global parametrization of Varner *et al.* [37], while the α-^{29}Si one was adopted from the scattering studies of Wühr *et al.* [38]. The wave function of the ^{5}Li ground state used in the single folding calculations was obtained by means of the CDCC technique, assuming that this state is a resonance located at 1.69 MeV above the $\alpha+p$ breakup threshold with a 1.25 MeV width [39]. The $\alpha+p$ binding potential had the same geometry as the potential for ^{5}He reported by Band and Ginoux [40]. The neutron binding potentials to the ^{5}Li and ^{28}Si cores were of standard W-S geometry with parameters radius $R = 1.25A^{1/3}$ fm and diffusivity $a = 0.65$ fm. The spectroscopic factors for ^{6}Li $= {}^{5}$Li+n were taken from the shell model prediction of Cohen and Kurath [41]. For the states in the final nucleus, the quantum numbers and spectroscopic factors were taken from (d, p) studies [36].

The calculated cross sections for all ten excited states of ^{29}Si were summed. The cross sections for the states with excitation energies larger than 2.43 MeV are weighted with the γ-ray branching ratios [42]. Final results of the calculations for the two incident energies are presented in Fig. 4.

B. *p* transfer

In the experiment, the emitted α's (^{6}Li+^{28}Si $\rightarrow$ ^{29}P+α + n) are measured in coincidence with γ's emitted from the first excited state of the final nucleus (3/2+ at 1.38 MeV). To reproduce these data, we studied one-proton transfers to five excited states of the final nucleus, the one listed above and four at higher excitation energies that subsequently γ-decay to the first excited state. For the calculations, the states with the highest spectroscopic amplitudes were chosen [43].

The parameters used in the DWBA calculations are as follows. Entrance channel potentials were calculated as described for the n transfer. The potentials in the exit channel were derived from neutron-^{29}Si and α-^{29}Si optical model potentials at relevant energies in a similar way as in n transfer. The neutron-^{29}Si potential was taken from the global parametrization of Varner *et al.* [37], while the α-^{29}Si was adopted from the scattering studies of Wühr *et al.* [38]. The wave function of the ^{5}He ground state used in the single folding calculations was obtained by means of the CDCC technique, assuming that this state is a resonance located at 0.8 MeV above the $\alpha+n$ breakup threshold and with 0.6 MeV width [39]. The $\alpha+n$ binding potential was taken from Bang and Ginoux [40]. The proton binding potentials to the ^{5}He and ^{28}Si cores were of standard W-S geometry with parameters $R = 1.25A^{1/3}$ fm and $a = 0.65$ fm. The spectroscopic factors for $^6\text{Li} = {}^5\text{He}+p$ were taken from the shell model prediction of Cohen and Kurath [41]. For the states in the final nucleus, the quantum numbers and spectroscopic factors were taken from proton stripping studies (τ, d) [42,43].

The calculated cross sections for the five excited states of ^{29}P were summed. The cross sections for the states with excitation energies larger than 2.43 MeV are weighted with the γ-ray branching ratios. Since the branching ratios for ^{29}P are not known, we performed two calculations for the beam energy of 13 MeV: one with branching ratios adopted from the corresponding levels of ^{29}Si [42] (see Fig. 1) and a second one with branching ratios set to unity. Final results of the first calculation are presented in Fig. 4, while the second is considered as an upper limit (see Table I). For 9 MeV, most of the calculated cross section comes from direct transfer to the first excited state, so the results do not depend on the branching ratios.

C. α transfer

In the experiment, the emitted protons were measured in coincidence with γ's emitted from the first excited state of the final nucleus (2+, 2.24 MeV, Fig. 5). This state can by reached by direct α transfer and by a transfer to the higher excited state of ^{32}S that subsequently decays to this state. It is well known that α-transfer reactions proceed mainly to the highly excited states of the final nucleus, close to the α barrier defined as $B = E_\alpha + V_C$, where V_C is the Coulomb barrier for the α-core nucleus (^{28}Si in our case) and E_α is the binding energy of α in the final nucleus (^{32}S) [44]. In ^{32}S, the excited state at 8.50 MeV, above the $^{32}\text{S} \rightarrow \alpha+{}^{28}\text{Si}$ breakup threshold, is known to have an α-cluster structure. It is strongly populated in ^{28}Si(^{6}Li, d)^{32}S reaction investigated by Tanabe *et al.* [45] at 75.6 MeV bombarding energy. Taking into account that this state decays by 33% to the first excited state of ^{32}S [46], the experimental results could correspond to the sum of transfers to the 2.24 MeV and by 33% to the 8.5 MeV state. However, we have no experimental evidence from our γ spectra that the last state is reached because of the low efficiency of our detector with respect to the high γ rays deexciting this state.

Since protons are the detected particles in the present experiment, we assume that the α-transfer reaction populates unbound states of the deuteron, above the $d \rightarrow n+p$ breakup threshold. Therefore, the DWBA calculations are performed for states in the $n+p$ continuum. The continuum is divided into bins of 1 MeV width up to an excitation energy of 10 MeV above the breakup threshold.

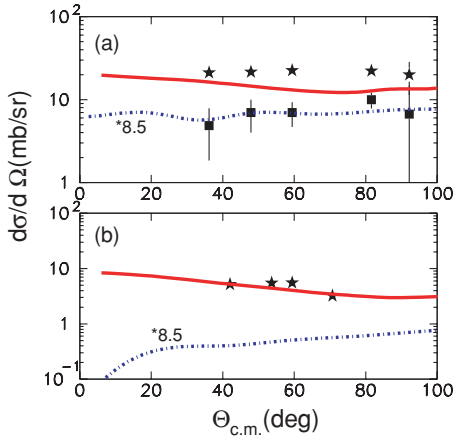

FIG. 5. (Color online) Experimental angular distributions (proton-γ coincidence measurements) with compound and transfer calculations (see text) for the $^6\text{Li}+{}^{28}\text{Si} \rightarrow {}^{32}\text{S}+p+n$ reaction at (a) $E_{\text{beam}} = 13$ and (b) $E_{\text{beam}} = 9$ MeV. Stars represent the original data; squares, the new data (original data minus the compound cross sections). Solid lines represent our evaporation calculation; dotted-dashed lines, our DWBA calculation for α transfer. The transfer calculations had to be multiplied by a factor of 8.5 to best fit the data at 13 MeV. At 9 MeV the evaporation cross sections seem to reproduce well the data.

The parameters used in the DWBA calculations are as follows. Entrance channel potentials are calculated as described for n transfer. For the exit channel we used d+^{32}S optical potentials derived from the global prescription of Haixia An and Chonghai Cai [47]. The potential binding $\alpha + d$ was adopted from Kubo and Hirata [48], while the ^{28}Si+α binding potential was of W-S shape with geometry parameters $R = 3.95$ fm and $a = 0.73$ fm [45]. For $^6\text{Li} = \alpha + d$ the spectroscopic factor was set to unity. The cluster wave functions of $^{32}\text{S}_{2.24,8.5\text{MeV}}$ states were calculated assuming 5S and 5P quantum numbers for these configurations, respectively, and spectroscopic factors derived by Tanabe *et al.* [45]. The 8.5 MeV excited state is unbound, so its wave function was calculated assuming a very weak binding energy of 0.1 MeV. The final results of the calculations for the two incident energies are presented in Fig. 5. The results are multiplied by a factor of 8.5 in order to fit the data at 13 MeV.

V. DISCUSSION AND SUMMARY

We have measured α and proton angular distributions in coincidence with γ rays deexciting nuclei produced in the reaction ^{6}Li+^{28}Si at two near-barrier energies, namely, 13 and 9 MeV. The coincidence requirement excluded the observation of incomplete fusion in our measurements, simplifying our study to total cross sections consisting solely of complete fusion and transfer reactions. In general, incomplete fusion does not seems to be a major contributor in the presently

studied reaction with a light target, as may be verified from our γ spectra. Moreover, exclusive breakup was found previously to exhibit very low cross sections of the order of 30 mb for $E_{\text{proj.}} = 13$ MeV. Therefore, in this study, transfer cross sections are determined taking into account total reaction cross sections and calculated fusion cross sections. A first indication of the quality of the fusion calculations is justified by comparing calculations and present measurements on a reaction channel formed solely by a compound process. Calculations and measurements are found to be in good consistency.

Ratios of transfer to compound cross sections and ratios of transfer vs total reaction cross sections are also formed and are displayed in Tables I and II. The results support the existence of strong transfer channels which become stronger and stronger approaching the barrier from higher to lower energies. Therefore, a detailed mapping of transfer near and below the barrier is necessary in order to interpret coupled channel effects at the barrier such as the "new" phenomenon of the potential threshold anomaly seen for weakly bound nuclei and the enhancement of "fusion" cross sections at the barrier. Depending on the projectile and target where different reaction channels may be open and depending on the type of meauserement, the reported fusion cross sections may really represent total reaction cross sections, and therefore theoretical studies on coupled channel approaches have to take this fact into account.

The importance of transfer at near-barrier energies has also been noted in the past for reactions with stable nuclei [49–53], and their influence on transfer has been discussed. In fact, in Ref. [49], studying elastic, transfer, and fission reactions at near-barrier energies for the systems ^{16}O+^{208}Pb and ^{16}O+^{183}Ta, the authors report that the ratio of quasielastic (inelastic and transfer) to total reaction cross section increases approaching the barrier, up to ~50% for the Pb case and 25% for the Ta case. Of course, in these cases, inelastic is a major contributor, but still transfer is also a substantial one.

In Table I, our present total reaction and transfer cross sections are compared with previous values [1,34,35] and are found to be in very good consistency. It has to be noted that in both values of total and transfer cross sections determined presently, a breakup cross section was added equal to 30 mb [21]. A possible contribution due to d transfer is not considered.

An effort was also made to compare our transfer results with DWBA calculations. Angle-integrated values of the total cross section for n, p, and α transfer are shown in Table I, under the column $\sigma_D{}^{\text{th}}$, while angular distributions are compared with the data ("new data") in Fig. 4, for exit channels leading to ^{29}Si and ^{29}P. As can be seen, the shape of the experimental distributions is very well reproduced by theory. However, the theoretical strength is in general smaller than the experimental one. Specifically for n transfer (^{29}Si) the data can best be reproduced if the theoretical points are multiplied by a normalization factor of ~3.5 for 13 MeV and a factor of ~4.5 for 9 MeV. For p transfer (^{29}P) these factors are 2.2 and 4.5 for 13 and 9 MeV, respectively, if we take into account the first calculation. As will be seen, these normalization factors depend strongly on energy for proton transfer and to a lesser extend depend also on energy for the neutron transfer. For α transfer, observed only at 13 MeV, a multiplication factor of 8.5 is necessary. The above disagreement in a quantitative basis between the DWBA calculations and the data could partly be justified by the dependence of the DWBA calculations on the optical potentials in the exit channel, which present a strong energy dependence since the reactions are investigated at energies close to the Coulomb barrier. Moreover, the potentials are not known empirically, since the nuclei produced in the exit channels are radioactive, both of them for p transfer and one of them (^{5}Li) for n transfer, and therefore exit channel potentials are generated by means of single folding calculations.

Summarizing, in exclusive particle-γ measurements, strong transfer channels are observed and quantified, exhibiting an increasing trend as we approach the barrier. The most substantial transfer channels are found to be n and p transfer. α transfer is also determined, but its cross section is small and is observed only at 13 MeV. d transfer cannot be observed in the statistic limits of this study. Ratios of transfer to total reaction cross section are formed and found to amount to 24% and 36% for 13 and 9 MeV, respectively. In view of these results, coupled channel studies require the knowledge of a detailed mapping of transfer around the barrier. The transfer results are found to be in very good qualitative agreement with DWBA calculations, while no quantitative agreement is obtained which may be attributed to the unknown empirical potentials of the exit channel nuclei.

ACKNOWLEDGMENTS

We would like to gratefully acknowledge Nick Keeley (Andrzej Soltan Institute for Nuclear Studies and DSM/DAPNIA CEA SACLAY) for carefully reading this manuscript and Massimo Loriggiola (Laboratori Nazionali di Legnaro, Italy) for providing the silicon targets.

[1] A. Pakou *et al.*, Phys. Lett. **B556**, 21 (2003).
[2] A. Pakou *et al.*, Phys. Rev. C **69**, 054602 (2004).
[3] J. M. Figueira *et al.*, Phys. Rev. C **75**, 017602 (2007).
[4] N. Keeley *et al.*, Nucl. Phys. **A571**, 326 (1994).
[5] A. M. M. Maciel *et al.*, Phys. Rev. C **59**, 2103 (1999).
[6] I. Martel, J. Gomez-Camacho, K. Rusek, and G. Tungate, Nucl. Phys. **A605**, 417 (1996).
[7] M. S. Hussein, P. R. S. Gomes, J. Lubian, and L. C. Chamon, Phys. Rev. C **73**, 044610 (2006).
[8] J. J. Kolata *et al.*, Phys. Rev. Lett. **81**, 4580 (1998).
[9] C. Signorini *et al.*, Eur. Phys. J. A **2**, 227 (1998).
[10] M. Trotta *et al.*, Phys. Rev. Lett. **84**, 2342 (2000).
[11] C. Signorini *et al.*, Eur. Phys. J. A **10**, 249 (2001).
[12] E. F. Aguilera *et al.*, Phys. Rev. Lett. **84**, 5058 (2000).
[13] A. Pakou *et al.*, Phys. Rev. Lett. **90**, 202701 (2003).
[14] A. Di Pietro *et al.*, Phys. Rev. C **69**, 044613 (2004).
[15] N. Keeley and K. Rusek, Phys. Lett. **B375**, 9 (1996).
[16] K. Rusek, N. Alamanos, N. Keeley, V. Lapoux, and A. Pakou, Phys. Rev. C **70**, 014603 (2004).
[17] A. Pakou *et al.*, Phys. Rev. C **71**, 064602 (2005).

[18] R. Raabe *et al*., Nature (London) **431**, 823 (2004).
[19] C. Beck, N. Keeley, and A. Diaz-Torres, Phys. Rev. C **75**, 054605 (2007).
[20] C. Signorini *et al*., Phys. Rev. C **67**, 044607 (2003).
[21] A. Pakou *et al*., Phys. Lett. **B633**, 691 (2006).
[22] A. Navin *et al*., Phys. Rev. C **70**, 044601 (2004).
[23] V. Tripathi *et al*., Phys. Rev. C **72**, 017601 (2005).
[24] A. Shrivastava *et al*., Phys. Lett. **B633**, 463 (2006).
[25] D. M. De Castro Rizzo *et al*., Nucl. Phys. **A427**, 151 (1984).
[26] P. R. S. Gomes *et al*., Nucl. Instrum. Methods Phys. Res. A **280**, 395 (1989).
[27] CASCADE: A Nuclear Evaporation Code, see F. Puhlhofer, Nucl. Phys. **A280**, 267 (1979); M. N. Harakeh, extended version; D. Pierroutsakou (private communication).
[28] A. Gavron, Phys. Rev. C **21**, 230 (1980); **56**, 1613 (1997).
[29] A. Gilbert and A. G. W Cameron, Can. J. Phys. **43**, 1446 (1965).
[30] A. V. Ignatyuk, G. N. Smirenkin, and A. S. Tishin, Sov. J. Nucl. Phys. **29**, 450 (1979).
[31] R. Bass, Phys. Rev. Lett. **39**, 265 (1977).
[32] P. M. Endt, At. Data Nucl. Data Tables **26**, 47 (1981).
[33] M. Dasgupta *et al*., Phys. Rev. C **70**, 024606 (2004).
[34] M. Hugi *et al*., Nucl. Phys. **A365**, 173 (1981).
[35] A. Pakou *et al*., Nucl. Phys. **A784**,13 (2007).
[36] R. J. Peterson *et al*., Nucl. Phys. **A408**, 221 (1983).
[37] R. L. Varner *et al*., Phys. Rep. **201**, 57 (1991).
[38] W. Wühr *et al*., Z. Phys. **269**, 365 (1974).
[39] D. R. Tilley *et al*., Nucl. Phys. **A708**, 3 (2002).
[40] J. Bang and C. Ginoux, Nucl. Phys. **A313**, 119 (1976).
[41] S. Cohen and D. Kurath, Nucl. Phys. **A101**, 1 (1967).
[42] P. M. Endt, Nucl. Phys. **A521**, 1 (1990).
[43] W. W. Dykoski and D. Denhard, Phys. Rev. C **13**, 80 (1976).
[44] W. Z. Goldberg *et al*., Izv. Acad. Nauk SSSR **33**, 586 (1969).
[45] T. Tanabe *et al*., Phys. Rev. C **24**, 2556 (1981).
[46] M. Babilon, T. Hartmann, P. Mohr, K. Vogt, S. Volz, and A. Zilges, Phys. Rev. C **65**, 037303 (2002).
[47] Haixia An and Chonghai Cai, Phys. Rev. C **73**, 054605 (2006).
[48] K.-I. Kubo and M. Hirata, Nucl. Phys. **A187**, 186 (1972).
[49] F. Videbæk *et al*., Phys. Rev. C **15**, 954 (1977).
[50] E. Vulgaris, L. Grodzins, S. G. Steadman, and R. Ledoux, Phys. Rev. C **33**, 2017 (1986).
[51] J. Wiggins *et al*., Phys. Rev. C **31**, 1315 (1985).
[52] R. A. Broglia, C. H. Dasso, S. Landowne, and A. Winther, Phys. Rev. C **27**, 2433 (1983).
[53] M. Beckerman *et al*., Phys. Rev. Lett. **45**, 1472 (1980).